



Statistical relationship between mix properties and the interfacial transition zone around embedded rebar



Amit Kenny, Amnon Katz*

National Building Research Institute, Faculty of Civil and Environmental Engineering, Technion – IIT, Haifa 32000, Israel

ARTICLE INFO

Article history:

Received 29 October 2014

Received in revised form 5 March 2015

Accepted 5 April 2015

Available online 9 April 2015

Keywords:

Image analysis

ITZ

Steel

Reinforcement

Concrete composition

Statistical method

ABSTRACT

The relationship between concrete mix properties and the properties of the interfacial transition zone (ITZ) formed around embedded rebar was investigated. Multiple samples of various mix compositions and bar orientations were prepared so as to represent common concrete technology. Water-to-cement ratios varied from 0.40 to 0.65 and powder (cement + limestone filler) contents ranged from 362 kg/m³ to 564 kg/m³. Over 1300 BSE images of the steel–concrete interface were taken and analyzed automatically. Statistical methods were used to identify correlations between ITZ properties and mix composition or fresh mix properties.

A single large void was identified beneath all horizontal bars regardless of concrete composition. The ITZ around vertical bars was more uniform and extended around the entire rebar. No clear relationship was found between ITZ thickness and mix composition or fresh mix properties for either vertical or horizontal bar orientations. The degree of ITZ variability beneath horizontal bars clearly depends, however, on the bleeding properties of the mix. The distance from steel surface to the closest concrete solid, which influences the chemistry over the surface of the steel, is affected by precipitation of hydration products in horizontal bars, but not by mix composition.

© 2015 Elsevier Ltd. All rights reserved.

1. Introduction

The interfacial transition zone (ITZ) in concrete is a phenomenon whereby properties of the cement paste adjacent to a solid boundary, such as aggregate or rebar, deviate from those observed in the bulk paste [1]. The ITZ between steel rebar and the surrounding concrete influences the mechanical behavior [2] and durability [3–5] of reinforced concrete structures. Most ITZ studies investigated the interface between cement paste and aggregates. These studies found higher porosity in proximity to the aggregate surface than in the bulk paste. The width of the ITZ around aggregates was quantified and found to extend up to 100 μm [6]. Liao [6] also found that during the hydration of cement, calcium hydroxide and secondary cementitious compounds precipitate within the pores of the ITZ and reduce its porosity. This porosity is assumed to be the result of poor compaction of cement grain along the interface due to the wall effect and micro-bleeding beneath the aggregate [7]. During the first two months of hydration, the width of the high porosity region decreases from 100 μm to about 15 μm [6], with the formation

of different hydration products at each age, a phenomenon known as preferential precipitation [1,6,8,9].

The ITZ around aggregates is known to be controlled by changing the particle grading to include particles smaller than the cement grain. This leads to a denser ITZ, due to reduction of the wall effect, and also changes the concrete's rheological properties, especially its bleeding [10]. Decreasing the water/cement (w/c) ratio reduces ITZ porosity around aggregates; according to [11], when the w/c ratio is 0.40 or less, ITZ porosity equals that of the bulk. Aggregate size also influences the porosity around the aggregate: the larger the aggregate, the higher the porosity [11]. The above observations were made for aggregates that were much smaller than steel rebar and that were subjected to strong shear forces that develop while mixing them with the cement paste.

Since the rebar is at rest in the form during casting, the ITZ around it differs from the ITZ around aggregate and was found to have different properties [7,12,13]. Some investigators emphasized the differences between the ITZ formed around vertical bars versus horizontal bars. Specifically, the ITZ formed around vertical rebar tends to be uniform and dense, whereas that formed around horizontal rebar has two distinct zones: an upper zone, above the rebar, that is relatively dense, and a lower zone, beneath the rebar, that is relatively large and porous, often consisting of a single, large

* Corresponding author. Tel.: +972 4 8293124.

E-mail address: akatz@technion.ac.il (A. Katz).

pore. Such differences in the ITZ also lead to micro-level differences in the mechanical properties of the paste beneath and above the rebar [2]. The differences between the areas above and below the rebar are less pronounced in self-consolidating concrete (SCC) [2]. Consolidation and internal bleeding (upward movement of water over solid particles that move downward during the consolidation of fresh concrete) were indicated as the cause of this difference [2,3,7,14]. Despite the broad agreement regarding the causes of this phenomenon, little information is available on the effect of concrete ingredients or fresh mix properties on the properties of this zone.

It appears, however, that ITZ properties are influenced by the fresh mix properties, which in turn are affected by the mix composition. Water and high-range water-reducing admixtures both decrease the concrete's plastic viscosity and yield stress [15]. Increasing the water/binder (w/b) ratio reduces plastic viscosity and increases bleeding [16]. Limestone powder, plasticizers, viscosity modifying agents and w/b ratio were found to have a strong influence on grout bleeding [16]. Replacing cement with limestone filler is associated with increased bleeding. Plasticizer and viscosity agents exhibited opposite effects: at low w/b ratios, increased plasticizer content increased bleeding, while increasing viscosity agent content reduced bleeding. Opposite effects were found at high w/b ratios [16].

The spatial nature of the ITZ was investigated mainly by analyzing a relatively small number of images, taken along [4] or across [7,17] the steel–concrete interface. Diamond [18] emphasized the need for a large number of measurements, because “the variation within a given tier around the periphery of a grain are often as great as, or greater than, the mean ITZ effects as customarily measured”. This observation by Diamond [18] and by others [19,20] led some authors to emphasize the importance of automated image analysis in quantitative research [19,20]. Automated image analysis offers the ability to analyze a large number of images in a way that is unbiased by human perception, yielding reliable information that can be analyzed statistically.

A vast amount of work has been done to understand the nature of ITZ around aggregates, and some work has been done to investigate the ITZ around steel rebar. Nevertheless, very few of the works were quantitative, and the porosity around steel rebar has yet to be correlated with mix properties of regular concrete. This paper presents part of a comprehensive study aimed at identifying the influence of ITZ properties on steel corrosion and recognizing the major parameters that influence the formation of ITZ around reinforcing bars in commonly used concrete technology. It offers an unbiased statistical examination of the data and correlations

between the mix properties and the ITZ properties, which are relevant for corrosion susceptibility. The relationships were determined using statistical methods to obtain reliable information, in view of Diamond's statement regarding the variability of ITZ properties [18]. Relationships between mix composition and ITZ properties were derived from automated image analyses of images taken around the entire perimeter of rebars for a large number of different mixes. ITZ properties were determined using an automated procedure. Over 1300 images of 16 different mix compositions and two rebar orientations were analyzed. Details of the automated image analysis developed for this study can be found in [21].

2. Methods

Sixteen different concrete mixes were produced so as to create varying ITZ properties using common concrete practice, i.e. workable concrete with good cohesiveness. Two series of mixes were prepared: (1) no filler and varying w/c ratios ranging from 0.40 to 0.65. Cement content ranged accordingly from 345 kg/m³ to 527 kg/m³; (2) constant w/c ratio of 0.45 or 0.52 with varying powder content. Powder content (cement, filler, and fines in the aggregates) ranged from 135 l/m³ to 204 l/m³. Powder content was calculated based on volume to account for the different specific gravity of the cement, filler, and fines. Water–powder (w/p) ratio ranged from 0.91 to 1.36 (by volume). Workability ranged from a slump of 80 mm to 185 mm. In addition a quasi-SCC mix was produced with the lowest w/p ratio, so as to investigate the influence of rheological properties of the extreme case but note that this mix does not represent a common concrete technology. It should be noted that a water-reducing agent (WRA) was used in various dosages to keep the concrete in workable state. One mix (w/c = 0.40) was cast twice on different days and served as an indication of our control over the concrete production process. Table 1 presents a list of mix compositions. All mixes were cast with rebar mounted in both horizontal and vertical positions so as to obtain different ITZ structures around the rebar, as described in [7].

ITZ properties were quantified using automated analysis of back-scattered electron (BSE) microscopy images, as described in [21]. Correlation coefficients were analyzed to reveal correlations between mix contents and properties and ITZ properties.

2.1. Materials

- *Cement*: CEM I complying with EN 197:2000.
- *Coarse aggregates*: crushed dolomite, 0–9.5 mm.

Table 1
Mix compositions per 1 m³ of fresh concrete.

Mix	Water (kg)	Cement (kg)	Air ^a (l)	Coarse (kg)	Fine (kg)	Filler (kg)	WRA ^b (kg)	w/c (w/w)	w/p (v/v)
W40	211	527	20	1359	249	0	5.3	0.40	1.12
W40B2	211	525	23	1356	249	0	5.3	0.40	1.12
W45	207	475	22	1384	287	0	4.1	0.44	1.21
W45C04	211	468	13	1359	299	19	4.7	0.45	1.20
W45C08	221	491	22	1348	223	39	4.4	0.45	1.16
W45C12	224	496	18	1374	187	60	5.0	0.45	1.12
W45C16	213	473	19	1373	204	76	4.7	0.45	1.07
W45C20	212	470	19	1384	184	94	4.9	0.45	1.04
W50	199	428	18	1396	339	0	2.1	0.47	1.28
W52C08	218	419	5	1378	300	34	4.2	0.52	1.36
W52C12	214	411	15	1378	279	50	4.1	0.52	1.27
W52C17	205	393	0	1386	325	68	5.9	0.52	1.25
W52C54	179	345	9	1164	496	208	6.2	0.52	0.91
W55	210	381	13	1351	400	0	1.9	0.55	1.49
W60	221	367	9	1393	355	0	0.0	0.60	1.62
W65	235	362	6	1390	335	0	0.0	0.65	1.75

^a Calculated.

^b Polysulfonate-based water-reducing agent, except mix W52C54 where polycarboxylate-based water-reducing agent was used.

- *Fine aggregate*: natural quartz sand, fineness modulus 1.73.
- *Filler*: calcium carbonate powder, median size 2.3 μm (Avgil 510 by Microgil).
- *Rebar*: 12 mm smooth surface steel rebar conforming to IS 4466. All rebars were cleaned using a custom method to ensure uniformity of sample preparation.

2.2. Mix preparation

Coarse aggregate was mixed first with 70% of the water for 1 min and allowed to absorb water at rest for additional 5 min. Fine aggregate, cement, powder, remaining water, and admixture were then added and mixed for additional 3 min in a pan mixer. Compressive strength and bleeding were measured according to EN12390 (100 mm cube), and EN 480-4 (total volume of water accumulated above a volume of concrete and its rate of accumulation), respectively. Table 2 presents the properties of fresh and harden concrete mixes. Workability, as a rheological indicator, was measured using the slump test (EN 12350-2).

2.3. Specimen preparation

Specimens with horizontal or vertical plain 12 mm diameter rebar were prepared for each concrete mix. Concrete was consolidated by filling the mold half way, vibrating on a vibratory table,

filling the second half and vibrating again. Vibration was performed until first signs of bleed water were seen on the surface of the fresh concrete. Specimens were cured in water at 20 °C for one week followed by 21 days at 20 °C, 100% RH. Fig. 1 presents the specimens' dimensions.

Two samples of each rebar orientation were sectioned to obtain prisms measuring about 30 mm \times 30 mm \times 70 mm, with the rebar parallel to the longitudinal axis and approximately centered in the other directions. The prisms were then sliced through their centers, using a precision diamond saw, to obtain slices 5 mm thick. This thickness was chosen to reduce interference due to the preparation procedure.

The slices were oven dried at 105 °C, vacuum impregnated with epoxy, and then polished and gold coated. Horne et al. [7] reported that drying of the paste in sections cut along the steel rebar led to its retraction to a distance of up to 3 μm from the steel, but this distance was usually much smaller. In sections cut across the steel, drying shrinkage may induce some radial cracks; however, these were omitted from the analysis by the image analysis procedure.

2.4. BSE image acquisition

The scanning electron microscope (SEM) used was a JEOL 5300, operated in back-scattered electron (BSE) mode at 30 kV and WD 30. Magnification was set at 100 \times , a value at which each pixel in

Table 2
Concrete properties.

Mix	Compressive strength (MPa)			Slump (mm)	Bleeding		
	3 days	28 days	90 days		Duration (hr:min)	Total (l/m ³)	Rate (l/m ³ /h)
W40	42.6	55.7	64.8	100	5:10	3.97	1.34
W40B2	40.7	52.7	58.8	126	N/A	N/A	N/A
W45	40.8	58.7	66.3	142	5:50	5.24	1.47
W45C04	40.5	54.0	57.3	95	4:30	3.30	1.03
W45C08	39.2	52.8	60.7	96	3:50	3.37	1.42
W45C12	37.8	50.0	54.7	110	4:40	4.98	1.62
W45C16	38.9	50.9	60.3	75	4:55	4.03	1.29
W45C20	40.1	57.6	62.9	110	5:20	4.48	1.16
W50	36.0	47.6	50.8	80	4:00	5.52	2.49
W52C08	38.5	50.5	55.2	132	5:20	8.10	2.16
W52C12	35.2	48.3	53.9	185	5:00	9.72	2.70
W52C17	35.0	52.1	52.3	80	4:10	4.66	1.43
W52C54a	39.9	59.4	66.0	>200 ^a	6:55	1.15	0.30
W55	29.4	47.9	51.2	122	4:55	9.32	2.27
W60	25.5	40.9	45.5	144	5:45	16.32	4.69
W65	21.4	40.1	41.0	170	5:10	26.69	6.41

^a A quasi-SCC mix. U box time – 5 s, L box time – 3 s, slump flow – 840 mm. For statistical calculations, slump was taken as 300 mm.

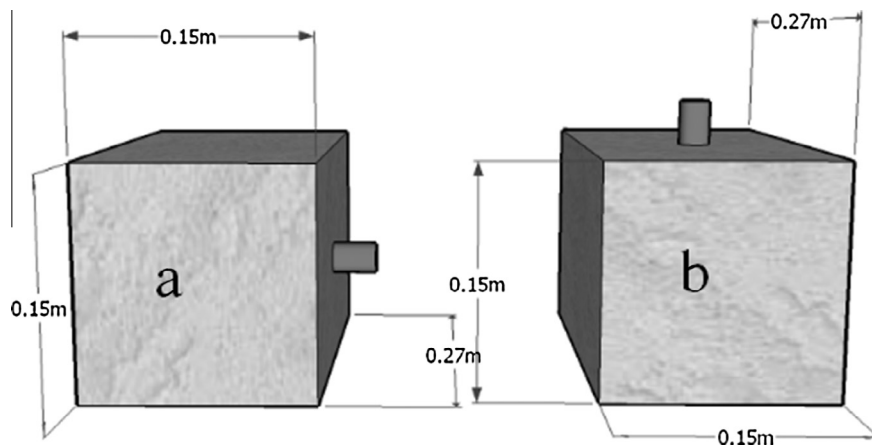


Fig. 1. Concrete specimens for ITZ investigations. (a) Horizontal-rebar specimen and (b) vertical-rebar specimen.

the digital image corresponds to an area of approximately $0.65 \mu\text{m} \times 0.65 \mu\text{m}$. This magnification value was chosen as a compromise between the need to include a full view of the large pores, on the one hand, and the desire to preserve adequate resolution of the smaller pores, on the other hand. Images were taken at fixed intervals around the rebar to obtain an unbiased representation of the ITZ. Two sections were taken for every rebar orientation of every concrete mix. A total of ~ 1300 images were taken.

2.5. ITZ characterization

The BSE images were analyzed automatically to obtain values for the following properties, for each image separately: ITZ thickness, porosity of this ITZ and steel–concrete distance. Statistical data (maximum, average, and standard deviation) were collected for each mix and rebar orientation. Since the ITZ is a highly variable entity, its variability, represented by the standard deviation, adds important information to the other statistical data (maximum and average); indeed, it can allude to the probable maximum value of the studied property along the entire rebar. A special, automated procedure of image analysis was developed as part of this study and is described in full in [21], yet a significant amount of manual work was required for image preparation (sectioning, polishing and microscopy).

In brief, BSE image yields an image with the various phases characterized by a different level of gray. A histogram of the gray levels of an image can represent the different phases but assigning each pixel to a specific phase is more complicated due to overlapping of the histograms from the various phases. Thus clustering the pixels based on the gray level threshold alone was found insufficient. Instead, the mean-shift clustering technique [22] was found to be more effective. Once the phases of interest were identified (concrete solids, steel and voids) determination of ITZ thickness, steel–concrete distance and porosity could be made.

2.6. Data analysis

Data analysis was performed using an objective statistical tool to verify relationships between mix composition or fresh mix properties and ITZ variables. Two parameters were calculated: correlation coefficient and p -value.

The correlation coefficient reflects the noisiness and direction of a relationship between two parameters. Here it was used to

indicate the existence or absence of relationships between the investigated variables. No correlation exists when the coefficient equals or is close to zero, and good correlation is indicated when the coefficient is close to 1 or to -1 for direct or inverse correlations, respectively. Although the correlation coefficient may clearly indicate the tendency, as long as the relationship is monotonous, it tells us nothing about the relationship type (e.g. linear or logarithmic). Eq. (1) describes the relationship between the correlation coefficient and the covariance:

$$R_{(i,j)} = \frac{C(i,j)}{\sqrt{C(i,i)C(j,j)}} \quad (1)$$

where $R_{(i,j)}$ is the correlation coefficient of the vectors i and j , $C_{(i,j)}$ is the covariance of the vectors i and j , and $C_{(i,i)}$ and $C_{(j,j)}$ are the covariances of each of the vectors with itself [23].

The p -value was used here to validate the significance of the correlations coefficients. The p -value represents the probability of obtaining a correlation coefficient from random data that is at least as valid as the p -value calculated for experimental data. P -values smaller than 0.05 represent confidence of more than 95% that the correlation is statistically significant. Statistical methods are frequently used in concrete studies to determine the significance of correlations among variables that cannot be isolated and identified separately [24–26].

3. Results and discussion

The ITZ around horizontal rebars comprises three distinctive regions: the region above the rebar, the region below the rebar, and the transition region between these two regions (Fig. 2a). The ITZ around vertical rebar is more uniform, with some arbitrary air pockets in contact with the rebar surface (Fig. 2b). Particles near the rebar surface are often graded: aggregates closer to the surface are smaller, usually of sub-millimeter size, and are larger, up to 3 mm in size, farther away from the rebar (Fig. 3a). Regions with larger aggregates rarely enter into the picture frame in the images used in this study. In several images, the ITZ around vertical rebars and above horizontal rebars is so thin that it is barely visible (Fig. 3b). Images in which large voids are found close to the rebar surface usually show a thin layer of solids on the rebar surface itself. Three types of solids can be identified upon visual inspection: (i) adhered cement paste (Fig. 3c – the brighter particles are of higher density and hence are identified as the remains of cement

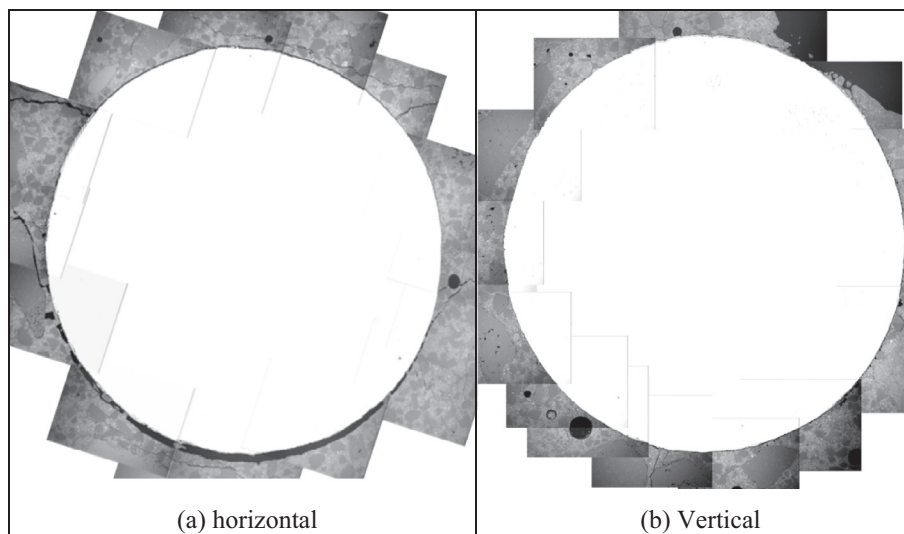


Fig. 2. ITZ around rebar.

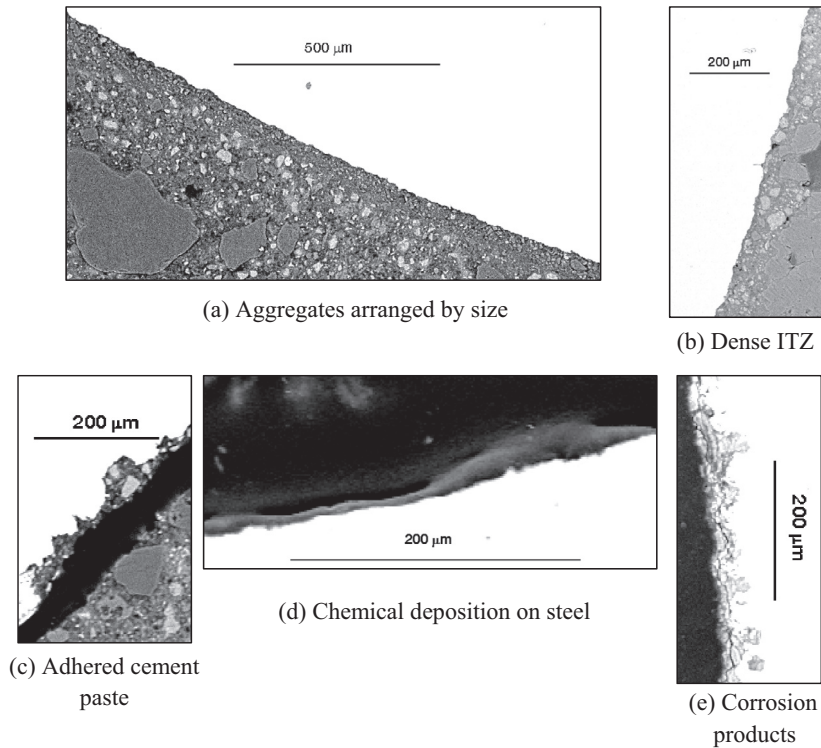


Fig. 3. Common phenomena in the ITZ (steel-white zone).

grains); (ii) thin low-density deposits, which do not contain granular matter (Fig. 3d); and (iii) corrosion products originating from the steel (Fig. 3e).

Although the rebar surface seems smooth to the naked eye, it is in fact irregular to the order of up to 10 μm . Many local pits were identified over the entire surface with the shallow pits usually filled with solids (see Fig. 3c–e).

3.1. ITZ properties

Table 3 presents ITZ properties for each mix and rebar orientation. For horizontal rebar, the values represent the property at the top and bottom of the rebar (average of 4–5 mm along the perimeter), due to the significant difference between the two zones. For vertical rebar, the property listed in the table represents the average of all images taken around the rebar. Table 4 presents the

standard deviation of the results. As is common in concrete microstructure, the standard deviation is relatively high and can indicate extreme values that may be obtained in extreme cases.

As can be seen in Fig. 4, the porosity found beneath all horizontal rebar was 1.0 or very close to this value; only mixes with a w/c of 0.52 and higher powder contents had a somewhat lower porosity of 0.8–0.9. The porosity above horizontal rebars and around vertical rebars ranged from 0.15 to 0.52 and from 0.24 to 0.46, respectively.

The results for ITZ thickness reveal similar trends: ITZ thickness below horizontal rebars is significantly greater than above horizontal rebars or around vertical rebars (Fig. 5). ITZ thickness of $\sim 100 \mu\text{m}$ was measured above horizontal rebars and around vertical ones, compared with $\sim 300 \mu\text{m}$ measured below horizontal rebars. A decrease in thickness was detected below horizontal bars at w/c = 0.52 when the powder content increased, until reaching a

Table 3
ITZ properties by concrete mix.

Mix	Porosity			ITZ thickness (μm)			Steel–concrete distance (μm)		
	Horizontal-bottom	Horizontal-top	Vertical	Horizontal-bottom	Horizontal-top	Vertical	Horizontal-bottom	Horizontal-top	Vertical
W40	1.00	0.48	0.34	268	106	112	1.98	1.66	1.65
W45	0.96	0.16	0.46	280	45	79	4.85	1.93	2.92
W45C04	0.96	0.52	0.40	245	88	89	3.34	2.50	1.86
W45C08	1.00	0.39	0.41	299	129	113	1.68	1.13	1.10
W45C12	1.00	0.23	0.24	311	114	136	5.27	1.48	1.23
W45C16	0.99	0.29	0.31	287	74	84	1.98	0.95	0.73
W45C20	1.00	0.49	0.28	304	87	76	13.38	3.21	2.34
W50	1.00	0.15	0.35	320	94	109	15.53	2.99	1.41
W52C08	0.97	0.21	0.46	288	81	135	2.91	2.84	1.41
W52C12	0.80	0.22	0.35	226	77	118	1.63	1.16	1.21
W52C17	0.92	0.20	0.36	186	85	85	14.91	1.46	1.65
W52C54	0.84	0.32	0.35	102	91	141	4.32	2.27	1.28
W55	0.99	0.21	0.30	264	104	117	2.00	1.69	0.75
W60			0.33			88			1.61
W65	0.90	0.15	0.30	296	54	110	1.80	0.89	1.08

Table 4
Standard deviation of ITZ properties.

Mix	Porosity			ITZ thickness (μm)			Steel–concrete distance (μm)		
	Horizontal-bottom	Horizontal-top	Vertical	Horizontal-bottom	Horizontal-top	Vertical	Horizontal-bottom	Horizontal-top	Vertical
W40	0.01	0.22	0.24	80	60	47	0.83	1.19	1.36
W45	0.06	0.09	0.24	56	13	45	4.21	1.30	1.69
W45C04	0.06	0.39	0.18	46	20	44	4.38	3.05	1.13
W45C08	0.02	0.13	0.12	95	58	36	1.60	0.64	0.58
W45C12	0.00	0.15	0.12	72	88	73	1.15	0.51	0.33
W45C16	0.00	0.16	0.05	35	20	37	0.06	0.23	0.15
W45C20	0.00	0.31	0.14	47	60	51	1.35	2.11	1.01
W50	0.00	0.08	0.10	28	40	66	13.7	1.20	0.45
W52C08	0.07	0.14	0.22	53	31	80	1.36	1.06	0.91
W52C12	0.18	0.10	0.16	84	49	65	0.91	0.52	0.78
W52C17	0.13	0.12	0.13	18	43	43	15.5	0.77	1.04
W52C54	0.19	0.19	0.13	35	73	49	3.24	1.13	0.58
W55	0.01	0.07	0.11	61	37	45	1.5	1.07	0.10
W60			0.14			43			0.94
W65	0.12	0.08	0.14	136	26	44	1.08	0.20	0.82

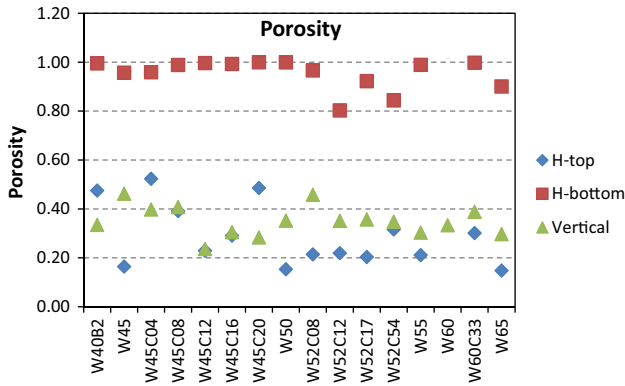


Fig. 4. ITZ porosity around horizontal (top and bottom) and vertical rebars.

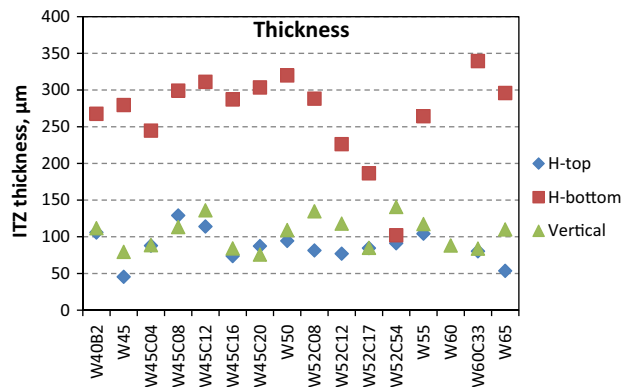


Fig. 5. ITZ thickness around horizontal (top and bottom) and vertical rebars.

value of 102 μm for mix W52C54 – a semi SCC mix. This value is in the range of ITZ thickness found around vertical bars and above horizontal bars. Since the objective of this paper is to evaluate ordinary concrete technology and since SCC represents a different concrete technology, this result was excluded from the statistical analysis in what follows. As opposed to this finding, increasing powder content of mixes with w/c = 0.45 had no effect on ITZ thickness under horizontal rebars, although powder content at this w/c was not tested to the same extent.

Steel–concrete distance displayed quite similar behavior, i.e. similar distances were measured around vertical bars and above

horizontal rebars while distances below horizontal rebars were greater (Fig. 6), although the difference between the two distinct zones was smaller than for ITZ thickness. No effect of powder content on steel–concrete distance was observed, unlike ITZ thickness below horizontal bars at w/c = 0.52, as described previously.

The differences between ITZ properties around vertical rebars and above horizontal bars were very small, and so they were tested statistically using a *t*-test to determine whether or not the results are statistically different. *T*-test values of 0.106, 0.006 and 0.306 were obtained for porosity, ITZ thickness, and steel–concrete distance, respectively. A value of 0.05 is generally considered as a criterion for significant confidence that the two sets of results are different; thus, it is clear that the difference between ITZ thickness around vertical rebar and above horizontal rebar is significant, but not for the porosity and steel–concrete distance.

It appears that mix composition in regular concrete technology has very little effect on ITZ properties around vertical or horizontal mounted rebars, but this conclusion is vague due to large variation in the results, thus it will be re-examined in what follows, using statistical means.

3.2. Relationships among mix properties

Mix compositions and properties of the fresh concrete are usually interdependent, making it more complicated to derive clear conclusions about the parameters influencing ITZ properties. When two properties are correlated with each other, it may appear as if both influence a certain ITZ property whereas only one of them is the real influencing parameter. Hence, it is essential to

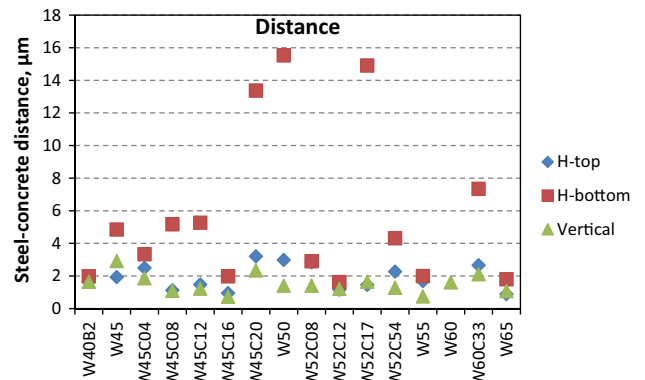


Fig. 6. Steel–concrete distance in horizontal (top and bottom) and vertical rebars.

conduct prior analysis of the relationship between mix compositions and fresh concrete properties. In addition, some of these correlations are quite obvious (e.g. cement content, which constitutes the major component of powders in the mix, is obviously correlated with powder content). Thus, these correlations were used here to validate the use of the proposed statistical tool to analyze the test results. Table 5 presents the correlation coefficients between mix compositions and properties of the fresh concrete. Correlations for which statistical confidence was greater than 95% (p -value < 0.05) are emphasized and the discussion in the followings refers only to these values.

The concrete mix exhibited the expected correlations between its constituents. Powder content was correlated with cement content (+0.64) because cement is the main powder component in the mixes; powder and cement contents were inversely correlated with the w/c ratio (−0.76 and −0.89, respectively) because more cement usually means a lower w/c ratio. Increasing powder content required an increase in the water reducing agent (WRA) content in order to maintain concrete workability, as reflected by a correlation coefficient of 0.83. As expected, slump was correlated with water content (+0.50) and with w/c and w/p as well (+0.53 and +0.56, respectively). These correlations are not considered “strong” due to the use of WRA, whose content is strongly correlated with the w/c and w/p ratios (−0.71 and −0.90, respectively). Some of these obvious correlations yielded fair values only due to the use of powders and WRA to control the fresh properties of the mixes; however, despite these concealing parameters, all “obvious” correlations were identified. These findings validate the use of the statistical method to identify relationships between the variables studied here.

Total bleeding and bleeding rate are collinear (0.98), i.e. an increase in one is accompanied by a proportional increase in the

other. Both, however, are not correlated with bleeding duration i.e. longer bleeding time is not necessarily accompanied by a larger volume of bleed water. In addition, the bleeding parameters, total bleeding and bleeding rate, are strongly correlated with both w/c and w/p (0.85, 0.82 and 0.90, 0.90, respectively); thus, as generally known in field practice, increasing cement or powder content reduces bleeding, but without any differentiation between the parameters (rate, duration, and total bleeding). This decrease in the bleeding rate and quantity brought about by increasing powder content is expected since powders supply more surface area for friction, which in turn restrict water movement between the particles. The correlation between bleeding parameters and the slump is not as strong as their correlation with w/c and w/p, i.e. more fluid concrete leads to more bleeding (total and rate) but this correlation is not as strong as the correlation with mix ingredients (~0.6 vs. ~0.9).

WRA reduce friction between powder particles and enable them to be packed more densely. Water that is displaced from the denser bulk may be the source of the greater volume of bleed water accompanied by relatively high correlation coefficient between bleeding and WRA (−0.85). Another interesting aspect of the intensive use of WRA is the lack of correlation between water content and water–cement ratio. In traditional concrete technology, high water content is usually associated with a high w/c value. Flexible use of WRAs as commonly used today breaks the link between the two.

3.3. Relationships among ITZ and mix properties

Table 6 presents correlations between ITZ properties and mix properties (composition and fresh-mix properties) for horizontal and vertical rebars. Table 7 presents similar correlations but with

Table 5
Correlations among mix properties.

		Water	Cement	w/c	Powders	w/p	WRA	Slump ^a	Bleeding	
									Total	Rate
Water		1.00	0.18	0.28	−0.29	0.60	−0.50	0.50	0.64	0.64
Cement		0.18	1.00	−0.89	0.64	−0.52	0.48	−0.40	−0.52	−0.48
w/c		0.28	−0.89	1.00	−0.76	0.79	−0.71	0.53	0.84	0.80
Powders		−0.29	0.64	−0.76	1.00	−0.93	0.83	−0.45	−0.75	−0.77
w/p		0.60	−0.52	0.79	−0.93	1.00	−0.90	0.56	0.90	0.91
Slump ^a		0.50	−0.40	0.53	−0.45	0.56	−0.46	1.00	0.69	0.64
Bleeding	Total	0.62	−0.57	0.85	−0.76	0.90	−0.85	0.64	1.00	0.98
	Rate	0.62	−0.54	0.82	−0.78	0.90	−0.89	0.57	0.98	1.00
	Duration	−0.36	−0.39	0.24	0.05	−0.10	0.03	0.59	0.09	0.00

Correlations with p -value below 0.05 are emphasized.

^a The quasi-SCC mix, W52C54, was not included for correlation with slump.

Table 6
Correlation between the ITZ and the mix properties.

Property			Mix content			w/c	w/p	Slump	Bleeding		
			Water	Cement	Powders				Total	Rate	Duration
Porosity	Horizontal	Bottom	0.24	0.63	0.18	−0.49 [*]	−0.08	−0.76	−0.26	−0.21	−0.18
		Top	−0.09	0.52 [*]	0.61	−0.62	−0.53	−0.15	−0.47 [*]	−0.52 [*]	−0.27
	Vertical		−0.18	0.05	−0.14	−0.13	−0.02	0.03	−0.21	−0.20	−0.13
ITZ thickness	Horizontal	Bottom	0.30	0.31	−0.20	−0.10	0.04	−0.07	0.10	0.16	0.14
		Top	−0.04	0.39	0.36	−0.40	−0.36	−0.48	−0.47 [*]	−0.42	−0.63
	Vertical		−0.10	−0.20	0.02	0.14	−0.05	0.49 [*]	0.00	−0.02	−0.02
Steel–concrete distance	Horizontal	Bottom	−0.34	−0.07	0.04	−0.05	−0.18	−0.29	−0.24	−0.16	−0.38
		Top	−0.43	0.01	0.10	−0.20	−0.26	0.00	−0.36	−0.35	−0.16
	Vertical		−0.16	0.29	0.14	−0.33	−0.20	−0.05	−0.21	−0.22	0.08

Correlations with p -value below 0.05 are emphasized.

^{*} Denotes 0.05 < p -value < 0.10.

Table 7

Correlation between the standard deviation of ITZ properties and the mix properties.

Property			Mix content			w/c	w/p	Slump	Bleeding		
			Water	Cement	Powders				Total	Rate	Duration
Porosity	Horizontal	Bottom	-0.30	-0.70	-0.21	0.53	0.08	0.76	0.23	0.16	0.15
		Top	-0.12	0.41	0.55	-0.52*	-0.49*	-0.12	-0.42	-0.48*	-0.20
	Vertical		0.03	0.23	-0.07	-0.21	0.02	0.14	-0.03	-0.07	0.28
ITZ thickness	Horizontal	Bottom	0.83	-0.11	-0.23	0.40	0.52*	0.66	0.70	0.68	0.53
		Top	-0.18	0.37	0.48*	-0.30	-0.36	-0.11	-0.24	-0.20	-0.34
Steel–concrete distance	Horizontal	Bottom	-0.41	-0.24	-0.27	0.10	0.02	-0.26	-0.18	-0.09	-0.49*
		Top	-0.30	0.21	0.15	-0.38	-0.27	-0.11	-0.39	-0.43	-0.15
	Vertical		0.01	0.22	-0.03	-0.19	0.00	0.02	0.00	-0.02	0.20

Correlations with *p*-value below 0.05 are emphasized.* Denotes $0.05 < p\text{-value} < 0.10$.

the standard deviation of ITZ properties so as to identify the parameters that control the variability of the results. The ITZ around horizontal and vertical rebar was found to be influenced by several different parameters, as follows.

3.4. ITZ around horizontal rebar

3.4.1. ITZ thickness

ITZ thickness found in this work was greater than that usually found around small aggregates, but it is nevertheless in the range reported in the literature for ITZ around rebar [4,3,23]. The thickness of the ITZ below horizontal rebar represents the size of the large void located beneath the rebar (Fig. 7). This thickness could not be correlated with any fresh mix property or composition in the ranges tested in this work (Table 6). Note that results for the SCC mix were excluded from the analysis. The standard deviation of ITZ thickness below the horizontal rebars was relatively high and correlated well with the parameters related to bleeding (total, rate and duration, as well as water content, slump and w/p, Table 7). This indicates a dynamic mechanism for the formation of the ITZ below horizontal bars, which is influenced by the bleeding parameters.

ITZ thickness above the rebar is much smaller than that of the ITZ beneath the rebar. Correlation was found between the thickness above horizontal rebars and both bleeding duration and total

bleeding, but not with other mix parameters, although bleeding duration itself is correlated with the slump. The variability of ITZ thickness above the rebar is correlated only with powder content, but with a *p*-value of 0.08.

3.4.2. ITZ porosity

The porosity of the ITZ below the rebars is correlated with cement content, and is inversely correlated with slump (and more weakly with w/c). ITZ porosity above the rebars is correlated with powder content (and more weakly with cement content) and is inversely correlated with w/p and w/c, which were found previously to be correlated with powder and cement contents. Similar trends were identified for the standard variation of the porosity.

The large void beneath horizontal rebars is clearly caused by the combined action of solid particle settlement and upward movement of bleeding water until entrapment beneath the rebar [2,3,7,14]. It is, however, interesting to note that no correlation was found between void size and any of the fresh concrete properties or mix compositions, but its standard deviation is correlated with these variables. It is possible that during bleeding, water accumulates beneath the rebar until it finally breaks through, along the sides of the rebar, moving upwards toward the surface, thus emptying the water lens and reducing its thickness. This “break-through” pressure depends on the rheological properties

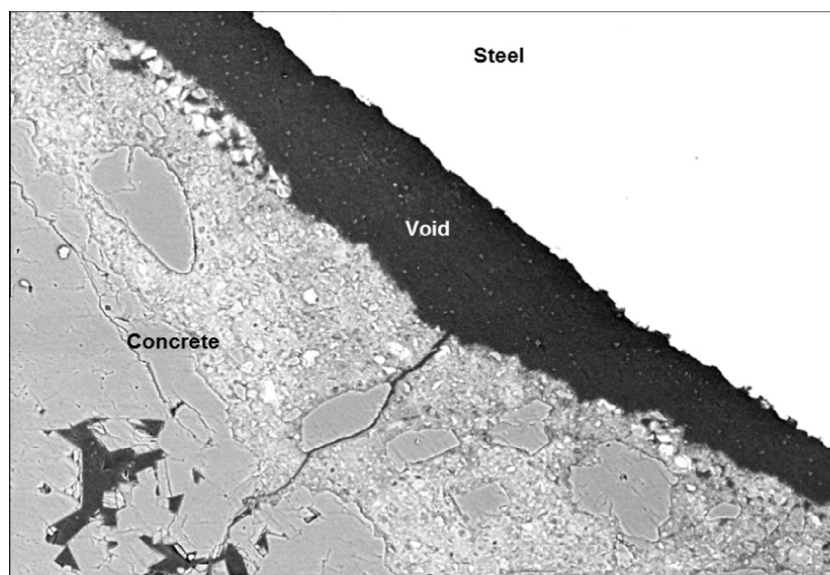


Fig. 7. BSE image of ITZ below horizontal rebar.

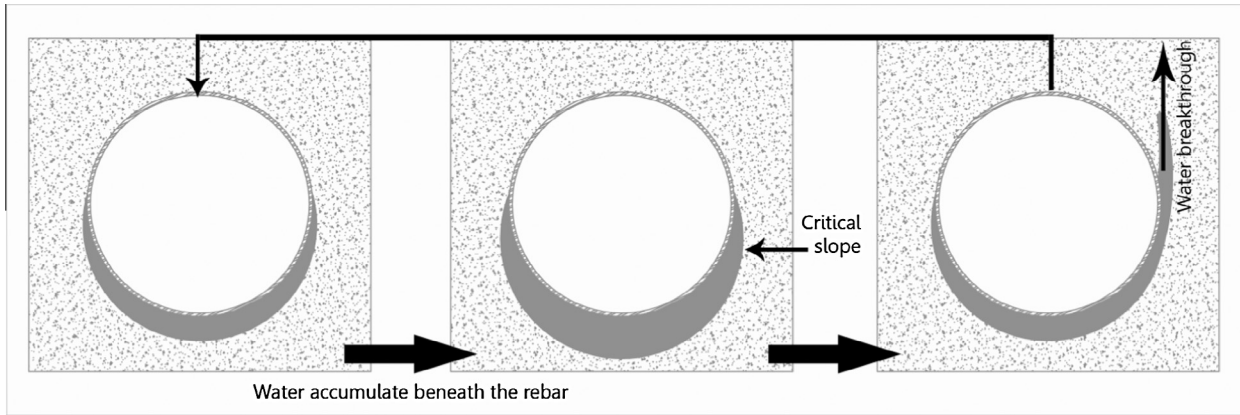


Fig. 8. Changes in ITZ thickness beneath horizontal rebar.

of the concrete surrounding the rebar and the process continues until the concrete hardens and prevents any more water from breaking through. The final shape of the void is determined and set at this point in time (Fig. 8). A higher volume of bleeding water or a higher rate of bleeding will obviously enhance this phenomenon, leading to more variation in the final ITZ thickness that will be expressed by higher values of standard deviation, as identified in this work.

On the upper side of the rebar, the ITZ is denser due to gradual settlement of the solid particles over the rebar. Longer settlement times, expressed by longer bleeding durations, probably lead to increased movement towards the rebar and to smaller ITZ thickness, expressed by a correlation value of -0.63 between settlement time and ITZ thickness.

3.4.3. Steel–concrete distance

No clear conclusions can be drawn as to which parameters affect the steel–concrete distance in the case of horizontal rebar. This small distance found in the images seems to be the result of either fine concrete components that adhere to the rebar surface or minerals that precipitate near the steel surface. Each of these mechanisms creates a different chemical environment on the steel surface that may affect corrosion initiation. Preferential deposition was found after splitting the concrete specimens used for the corrosion test (Fig. 9). Deposits and preferential deposition were found even on the steel surface in a model that simulated the ITZ between steel and cement paste [27]. Deposits of carbonate on metals are known to precipitate at oxygen reduction sites and have an inhibitive impact on oxygen reduction [28]. Hence, these observed deposits may play some role in the corrosion process. Additional chemical analysis is needed if the chemical composition of the particles is of interest.

3.5. ITZ around vertical rebar

The ITZ images taken around vertical rebar present a completely different picture (Fig. 2b): concrete and voids are evenly

distributed all around the rebar with no preference to a single void in a specific location, as was seen for the horizontal rebar.

3.5.1. Porosity, ITZ thickness and steel–concrete distance

No correlation was found between any of these parameters or their deviation and any of the mix composition parameters or fresh mix properties. It appears that practically, in regular concrete technology in the range of compositions tested in this study, it is impossible to control the properties of ITZ around vertical rebars. Note that due to similarity of the results for vertical rebars in mix W52C54 (quasi-SCC) to the results from the other mixes they were included in the statistical analysis.

4. Summary and conclusion

The correlation between ITZ properties around horizontal and vertical reinforcing bars and fresh mix properties or mix composition was studied for a wide range of concretes representing common concrete technology. One large void was identified below all horizontal rebars and a relatively dense structure was identified around all vertical rebars as well as above horizontal rebars.

ITZ thickness below horizontal bars ranged between $186\ \mu\text{m}$ and $320\ \mu\text{m}$ and it was not correlated with any of the mix compositions or fresh mix properties (i.e. slump and bleeding). It was found, however, that the greater the bleeding parameters, the larger the variation in the results. A mechanism was proposed according to which bleeding water that accumulates beneath the rebar rises along the side of the rebar and finds its way up. The final size of the void is determined randomly when continuous hydration prevents this movement. According to this mechanism, the void size is not related directly to the bleeding water volume. The rheological properties of the mix, e.g. viscosity, may play a role in determining the size of the void that develops before the water rises and the final void is formed.

The steel–concrete distance for horizontal rebar may be influenced by processes that occur during hydration and by adhesion of particles to the steel surface. Hence, for a constant concrete



Fig. 9. Rebar with worm-like deposits on its non-corroded part.

chemistry, as was maintained in this work, mix proportions may have an insignificant effect on steel–concrete distances in the case of horizontal rebar.

No clear relationship was found between ITZ parameters around vertical rebar and mix composition or fresh mix properties.

According to the results it appears that it is quite impossible to control the properties of the ITZ in the range of mix compositions studied in this work except for a quasi-SCC mix that exhibited smaller ITZ thickness below horizontal rebars. These ITZ properties are important in controlling the development of steel corrosion and so additional work is needed to gain a better understanding of ITZ formation around rebar, and of whether and how it can be controlled.

Acknowledgment

Partial support by the Israel-Germany Foundation (GIF) is gratefully acknowledged.

References

- [1] Diamond S, Huang J. The interfacial transition zone: reality or myth. In: Katz A, et al., editors. *The interfacial transition zone in cementitious composites*. E&FN Spon: Haifa, Israel, 1998. p. 3–39.
- [2] Zhu W, Sonebi M, Bartos PJM. Bond and interfacial properties of reinforcement in self compacting concrete. *Mater Struct* 2004;37(271):442–8.
- [3] Mohammed TU, Hamada H. A discussion of the paper “chloride threshold values to depassivate reinforcing bars embedded in a standardized OPC mortar” by Alonso C, Andrade C, Castellote M, Castro P. *Cem Concr Res* 2001;31(5):835–8.
- [4] Glass GK, Reddy B. The influence of the steel concrete interface on the risk of chloride induced corrosion initiation. *Corros Steel Reinf Concr Struct* 2002.
- [5] Castel A et al. Influence of steel–concrete interface quality on reinforcement corrosion induced by chlorides. *Mag Concr Res* 2003;55(2):151–9.
- [6] Liao K-Y et al. A study on characteristics of interfacial transition zone in concrete. *Cem Concr Res* 2004;34(6):977–89.
- [7] Horne AT, Richardson IG, Brydson RMD. Quantitative analysis of the microstructure of interfaces in steel reinforced concrete. *Cem Concr Res* 2007;37(12):1613–23.
- [8] Odler I. Hydration, setting and hardening of Portland cement. In: Hewlett PC, editor. *Lea's chemistry of cement and concrete*. Arnold: London; 1998. p. 241–98.
- [9] Bonen D. Features of the interfacial transition zone and its role in secondary mineralization. In: *The interfacial transition zone in cementitious composites*. Haifa, Israel: E and FN Spon; 1998.
- [10] Bentur A et al. Review of the work of the RILEM TC 159-ETC: engineering of the interfacial transition zone in cementitious composites. *Mater Struct/Mater Constr* 2000;33(226):82–7.
- [11] Elsharief A, Cohen MD, Olek J. Influence of aggregate size, water cement ratio and age on the microstructure of the interfacial transition zone. *Cem Concr Res* 2003;33:1837–49.
- [12] Glass GK et al. Backscattered electron imaging of the steel–concrete interface. *Corros Sci* 2001;43(4):605–10.
- [13] Koleva DA et al. Correlation of microstructure, electrical properties and electrochemical phenomena in reinforced mortar. Breakdown to multi-phase interface structures. Part II: Pore network, electrical properties and electrochemical response. *Mater Charact* 2008;59(6):801–15.
- [14] Neville AM. Properties of Concrete. In: 9th ed., England: Pearson; 2011. p. 809.
- [15] Hu C, de Larrard F. The rheology of fresh high-performance concrete. *Cem Concr Res* 1996;26(2):283–94.
- [16] Svermova L, Sonebi M, Bartos PJM. Influence of mix proportions on rheology of cement grouts containing limestone powder. *Cem Concr Compos* 2003;25(7):737–49.
- [17] Ujike I, Buenfeld NR. Development of a method quantifying entrapped air voids at steel–concrete interface in real structure, 2006. p. 119–28.
- [18] Diamond S. Considerations in image analysis as applied to investigation of the ITZ in concrete. *Cem Concr Res* 2001;23(2–3):171–8.
- [19] Chermant JL. Why automatic image analysis? An introduction to this issue. *Cem Concr Compos* 2001;23(2–3):127–31.
- [20] Scrivener KL. Backscattered electron imaging of cementitious microstructures: understanding and quantification. *Cem Concr Compos* 2004;26(8):935–45.
- [21] Kenny A, Katz A. Characterization of the interfacial transition zone around steel rebar by means of the mean shift method. *Mater Struct* 2012;45(5):639–52.
- [22] Shimshoni I, Georgescu B, Meer P. Adaptive mean shift based clustering in high dimensions. In: Shakhnarovich G, Darrell T, Indyk P, editors. *Nearest-neighbor methods in learning and vision: theory and practice*. MIT Press; 2006. p. 203–20.
- [23] Spiegel MR, Stephens LJ. *Theory and problems of statistics*. Schaume's outline series. McGraw Hill; 2008.
- [24] Ulloa VA et al. New views on effect of recycled aggregates on concrete compressive strength. *ACI Mater J* 2013;110(6):687–96.
- [25] Strauss A et al. Advanced life-cycle analysis of existing concrete bridges. *J Mater Civil Eng* 2008;20(1):9–19.
- [26] Parsekian GA et al. Properties of mortar using cubes, prism halves, and cylinder specimens. *ACI Mater J* 2014;111(4):443–54.
- [27] Kenny A. The micro structure of concrete around embedded steel influence on the chloride threshold for chloride induced corrosion. In: Faculty of Civil & Environmental Engineering, Technion – Israel Institute of Technology; 2011. p. 170.
- [28] Bockris JOM, Reddy AKN. *Modern electrochemistry*. Plenum Press; 1970. p. 810.